◆ Human Brain Mapping 33:2941–2956 (2012) ◆

Degeneration of Corpus Callosum and Recovery of Motor Function After Stroke: A Multimodal Magnetic Resonance Imaging Study

Ling E. Wang,[1,2,3,4] Marc Tittgemeyer,[3] Davide Imperati,[3] Svenja Diekhoff,[3] Mitra Ameli,[5] Gereon R. Fink,[1,5] and Christian Grefkes[1,3,5]*

[1]*Cognitive Neurology Section, Institute of Neuroscience and Medicine (INM-3), Research Centre Juelich, Germany*
[2]*International Graduate School of Neuroscience and Research School, Ruhr University Bochum, Germany*
[3]*Neuromodulation and Neurorehabilitation Section, Max Planck Institute for Neurological Research, Cologne, Germany*
[4]*Division of Speech and Hearing Sciences, Faculty of Education, The University of Hong Kong, China*
[5]*Department of Neurology, University of Cologne, Germany*

Abstract: Animal models of stroke demonstrated that white matter ischemia may cause both axonal damage and myelin degradation distant from the core lesion, thereby impacting on behavior and functional outcome after stroke. We here used parameters derived from diffusion magnetic resonance imaging (MRI) to investigate the effect of focal white matter ischemia on functional reorganization within the motor system. Patients ($n = 18$) suffering from hand motor deficits in the subacute or chronic stage after subcortical stroke and healthy controls ($n = 12$) were scanned with both diffusion MRI and functional MRI while performing a motor task with the left or right hand. A laterality index was employed on activated voxels to assess functional reorganization across hemispheres. Regression analyses revealed that diffusion MRI parameters of both the ipsilesional corticospinal tract (CST) and corpus callosum (CC) predicted increased activation of the unaffected hemisphere during movements of the stroke-affected hand. Changes in diffusion MRI parameters possibly reflecting axonal damage and/or destruction of myelin sheath correlated with a stronger bilateral recruitment of motor areas and poorer motor performance. Probabilistic fiber tracking analyses revealed that the region in the CC correlating with the fMRI laterality index and motor deficits connected to sensorimotor cortex, supplementary motor area, ventral premotor cortex, superior parietal lobule, and temporoparietal junction. The results suggest that degeneration of transcallosal fibers connecting higher order sensorimotor regions constitute a relevant factor influencing cortical reorganization and motor outcome after subcortical stroke. *Hum Brain Mapp 33:2941–2956, 2012.*

Key words: diffusion MRI; fMRI; motor deficits; corpus callosum; DTI

Additional Supporting Information may be found in the online version of this article.

*Correspondence to: Christian Grefkes, MD, PhD, Neuromodulation and Neurorehabilitation, Max Planck Institute for Neurological Research, Gleueler Str. 50, 50931 Köln, Germany.
E-mail: christian.grefkes@uk-koeln.de

Received for publication 24 January 2011; Revised 20 May 2011; Accepted 24 June 2011

DOI: 10.1002/hbm.21417
Published online 22 October 2011 in Wiley Online Library (wileyonlinelibrary.com).

INTRODUCTION

Focal brain lesions resulting from ischemia may trigger structural and functional changes in both gray matter and white matter [Cramer, 2008; Stinear et al., 2007]. Diffusion magnetic resonance imaging (MRI) studies in stroke patients have shown that the structural integrity of descending motor pathways (e.g., the corticospinal tract [CST]) may influence both functional reorganization of the motor cortex [Newton et al., 2006; Schaechter et al., 2008] and motor performance of the paretic hand [Jang et al., 2008; Lindenberg et al., 2010; Schaechter et al., 2009; Stinear et al., 2007; Thomalla et al., 2004; Yu et al., 2009]. For example, decreases in fractional anisotropy (FA), an index for directional diffusion of water molecules which is often used as an indicator for white matter integrity, in the ipsilesional CST significantly correlated with reduced motor skills of the affected hand of chronic stroke patients [Schaechter et al., 2009]. In addition to CST fibers, interhemispheric connections were suggested to play an important role in modulating activity in cortical motor areas and thereby motor performance of the affected hand in stroke patients [Grefkes and Fink, 2011; Grefkes et al., 2010; Hummel et al., 2005; Johansen-Berg et al., 2002; Mansur et al., 2005; Nowak et al., 2008]. Transcranial magnetic stimulation (TMS) studies revealed that motocortical excitability and modulation thereof is not only altered in the lesioned but also in the contralesional hemisphere remote from stroke lesions [Butefisch et al., 2003; Talelli and Rothwell, 2006]. Paired-pulse interhemispheric stimulation protocols demonstrated that some patients may show abnormally increased interhemispheric inhibition exerted by contralesional primary motor cortex (M1) on ipsilesional M1 during movement initiation of the affected hand [Murase et al., 2004]. Similar results were obtained from analyses of effective connectivity derived from functional magnetic resonance imaging (fMRI) data showing that the stronger movement-related inhibition from contralesional M1 the more pronounced are the motor deficits of the affected hand [Grefkes et al., 2008b].

Changes in white matter integrity after stroke may result from both axonal degeneration (due to neuronal damage) and demyelination (due to damage of oligodendrocytes) which can also be observed in regions distant to the primary ischemic lesion [Arai and Lo, 2009; Medana and Esiri, 2003; Valeriani et al., 2000; Wakita et al., 2002]. Loss of axonal integrity and myelin sheath interferes with neuronal connectivity within and across the hemispheres, and may hence be detrimental for recovery of function [De Stefano et al., 2001; Petzold et al., 2005; Volpe, 2001]. Recent animal studies investigating models of ischemia using diffusion MRI demonstrated that changes in parallel and perpendicular diffusivity can be linked to alterations of both axonal integrity and degradation of myelin [Budde et al., 2009; Song et al., 2003; Sun et al., 2008; Zhang et al., 2009]. Although the neurobiological mechanisms underlying changes in specific diffusion parameters are incompletely understood for the human brain, such an approach might allow a better understanding of the structure-function relationships underlying functional reorganization and recovery of function in patients suffering from brain lesions. We, therefore, used diffusion MRI (dMRI) and fMRI in stroke patients to test the hypothesis that changes in white matter diffusivity are associated with both functional reorganization within the cortical motor system and motor deficits in stroke patients. We furthermore hypothesized that functional reorganization between the hemispheres is related not only to structural abnormalities of the CST [Schaechter et al., 2009; Schaechter et al., 2008; Ward et al., 2006] but also to changes in transcallosal fibres among sensorimotor regions and that such damage might also influence motor outcome after stroke.

MATERIALS AND METHODS

The study was approved by the local ethics committee (file no. 06-209) and was conducted in accordance with the Declaration of Helsinki. Informed consent was obtained from each participant prior to the study.

Subjects

Eighteen first-ever stroke patients (see Table I for clinical details) with unimanual motor deficits due to subcortical ischemic lesions were recruited from the Department of Neurology, University of Cologne, Germany. Figure 1 depicts the lesion pattern of the patient sample. Patients were included in the study based on the following criteria: (i) strictly subcortical lesions and no leukoaraiosis as verified by structural MRI; (ii) unilateral hand motor deficits; (iii) absence of aphasia, neglect, and apraxia; (iv) no mirror movements of the unaffected hand. The following clinical scores were assessed: National Institutes of Health Stroke Scale (NIHSS), modified Rankin Scale (MRS), and Beck Depression Inventory (BDI, see Table I). These clinical scores were assessed on the day when patients were tested with d/fMRI. The initial NIHSS in the acute phase of the stroke and the type of treatment the patients received in the successive weeks are reported in Table I. Twelve (four female) healthy subjects (mean age $\pm$ SD: 62.5 $\pm$ 7.9 years) without any history of neurological, psychiatric, or orthopedic disease served as controls. According to the Edinburgh Handedness Inventory [Oldfield, 1971], all control subjects were right-handed. The presence of mirror movements was monitored by visual inspection of the hand muscles of the unaffected hand while patients tapped with their affected index finger at maximum speed. This setting, however, cannot exclude the possibility that some patients had minimal co-contractions.

Behavioral Assessments

The action research arm test (ARAT) was used to quantify motor deficits. The ARAT is an observational test of

TABLE I. Summary of patients' information

Patient No.	Age (yr)	Sex	Handedness[a]	Affected hand	Site of lesion	Lesion size (cm^3)	Lesion age (wk)	Medication	Rehabilitation	NIHSS[1]	NIHSS[2]	mRS	BDI	ARAT	fMRI laterality index
1	41	M	R	L	R BG/IC	1.03	12	ASA	6 wk Inp	6(2)	2(0)	1	3	53	0.17
2	54	M	R	R	L BG/CR	12.93	7	Thrombolysis, Phenprocoumon	6 wk Inp	11(3)	4(0)	1	4	54	0.50
3	35	F	R	R	L BG/CR/TH	32.89	2	ASA	6 wk Inp	10(2)	8(2)	3	4	27	0.12
4	55	F	L	R	L CR	1.50	25	ASA	6 wk Inp	6(1)	2(1)	2	7	55	0.55
5	46	M	R	L	R BG/CR	1.94	8	ASA	6 wk Inp	7(2)	5(1)	1	16	55	0.06
6	36	F	R	L	R CR	1.41	1	Thrombolysis, Clopidogrel	6 wk Inp	8(3)	3(0)	2	10	57	0.33
7	50	F	R	R	L Pons	1.15	8	ASA	3 wk Inp	5(1)	3(1)	1	2	56	0.44
8	55	M	R	L	R IC	1.17	46	ASA	6 wk Inp	7(2)	3(1)	3	17	31	−0.07
9	49	F	R	R	L CR	0.54	41	ASA	3 wk Outp	6(2)	5(0)	1	8	40	0.06
10	54	M	R	R	L CR	0.69	5	ASA	6 wk Inp	7(2)	3(0)	1	1	55	0.52
11	27	F	R	L	R BG/CR/TH	3.40	1	Clopidogrel	3 wk Outp	3(2)	2(1)	1	12	57	0.34
12	78	F	R	L	R TH	0.41	88	ASA	3 wk Inp	9(2)	4(1)	2	10	35	0.06
13	64	M	R	L	R CR	0.37	5	ASA	6 wk Inp	8(2)	1(1)	2	1	51	0.00
14	69	M	R	R	L BG/CR/IC/TH	21.63	5	ASA	4 wk Inp	--	5(1)	3	--	47	0.13
15	66	M	R	L	R BG/CR/TH	28.59	43	ASA	6 wk Inp	11(3)	5(2)	3	9	33	0.05
16	55	M	R	L	R BG/CR/TH	1.25	67	Phenprocoumon	6 wk Inp	--	1(1)	1	6	53	0.23
17	72	M	R	L	R TH	0.40	66	ASA, Dipyridamole	6 wk Inp	8(1)	2(0)	2	12	31	0.05
18	74	M	R	R	L TH	0.27	100	Clopidogrel	6 wk Outp	5(1)	1(0)	1	1	56	0.13
	54.4 ± 14.3	7 F/ 11 M	1 L/ 17 R	10 L/ 8 R			29.4 ± 32.2			7 [3, 11]	3 [1, 8]	1.5 [1, 3]	7 [1, 17]	53 [27, 57]	0.20 ± 0.19

[a]Handedness is determined according to the Edinburgh Handedness Inventory [Oldfield, 1971]. Abbreviations: ARAT, action research arm test; BDI, Beck Depression Inventory; mRS, modified Rankin score; NIHSS, National Institutes of Health Stroke Scale. NIHSS[1], these data were assessed at the acute hospital stage. NIHSS[2], the data were assessed on the day of the present experiment. The numbers in brackets indicate the NIHSS subscore for arm motor function. BG, basal ganglia; CR, corona radiata; IC, internal capsule; TH, thalamus. L, left; R, right. ASA, acetylsalicylic acid; Inp, inpatient rehabilitation clinic; Outp, outpatient rehabilitation facilities. --: unavailable data. See also Figure 1 for demonstration of lesion locations. The mean with standard deviation or median is given with range in square brackets.

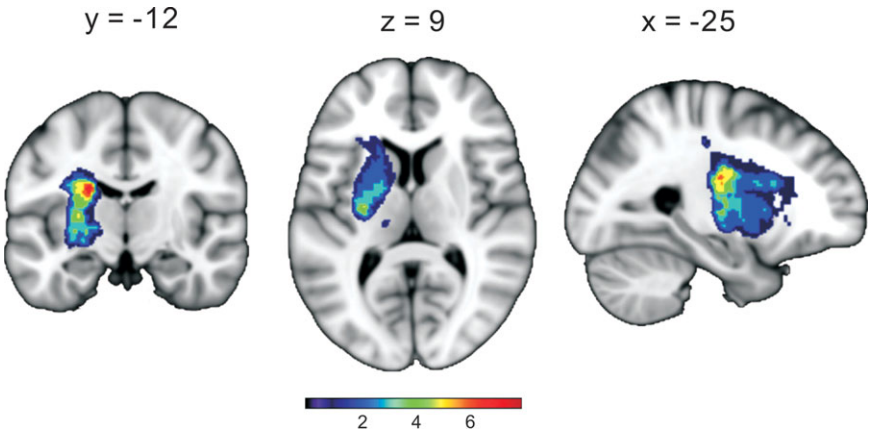

Figure 1.
Lesion map. The lesion mask of each patient (drawn on the respective T1-weighted images) was spatially normalized to and overlaid on a Montreal Neurological Institute (MNI) brain template. The color code indicates the degree of overlap across patients.

motor performance of the upper limb consisting of 19 items [Yozbatiran et al., 2008]. Performance of each item is scored on a 4-point scale ranging from 0 to 3 with higher scores denoting better motor performance (maximum overall score: 57). Each item was videotaped and rated by two experimenters (LW and CG).

Image Acquisition

All MRI data were acquired with a Siemens Trio 3.0 T whole body scanner (Erlangen, Germany).

Functional MRI

We used a gradient echo planar imaging (EPI) sequence to acquire fMRI data with the following parameters: repetition time (TR) = 2,250 ms, echo time (TE) = 30 ms, field of view (FOV) = 200 mm, 37 axial slices, slice thickness = 3.4 mm, distance factor = 15%, in-plane resolution = 3.1 × 3.1 mm^2, and flip angle = 90°.

The fMRI experiment consisted of an index finger-tapping task. Inside the MR scanner, subjects rested both hands with their palms pointing downwards on a small rubber panel (20 × 15 × 3 cm^3) placed upon the abdomen. Upon a visual cue, subjects performed index finger-tapping movements as fast as possible with the left or right hand. The instruction cue consisted of a black arrow pointing either left or right on a white background (duration was jittered between 3 and 4.5 s). The appearance of a red circle (for 4 s) at the center of the screen indicated to the subjects to start tapping with the left or right index finger. Three cycles of movements were separated by a 2-s pause to prevent muscular fatigue (total block length: 16 s). Movement blocks were separated by resting baselines (duration: 16 s) in which subjects were instructed to relax while watching a blank black screen. All visual stimuli were generated using the software "Presentation" (version 11.0, Neurobehavioral Systems, Albany, CA) and were displayed on a shielded thin film transistor (TFT) screen at the rear end of the scanner, visible via a mirror mounted on the headcoil. The whole experiment lasted approximately 11 min and involved a total of 20 task blocks separated by 20 resting (baseline) blocks. Prior to scanning, subjects were trained for 2–3 min so as to achieve a stable tapping performance in three successive blocks of trials. The motor performance (i.e., number of taps per block) of each patient was recorded by an experimenter standing inside the scanner room. No mirror movements were detected when patients moved either the affected or the unaffected hand.

Diffusion MRI

Diffusion MRI data were acquired using a spin EPI sequence with the following parameters: TR = 9,000 ms, TE = 87 ms, FOV = 220 mm, 72 axial slices, slice thickness = 1.7 mm, and in plane resolution = 1.7 × 1.7 mm^2. Diffusion weighting was isotropically distributed along 60 directions (b = 1000 s/mm^2). The acquisition of the diffusion weighted images was performed in blocks of 10 images with different diffusion directions and an additional image with no diffusion weighting (B0) (i.e., one B0 image per 10 diffusion weighted images). The B0 images served as anatomical reference for motion correction. The entire data acquisition protocol lasted around 10 min.

Structural imaging

At the end of the fMRI and dMRI sessions, anatomical scans (T1-weighted and fluid attenuated inversion recovery [FLAIR]) were acquired for detecting lesion location and anatomical reference (see Supporting Information Methods for detailed parameters).

Image Analysis

Prior to data analyses, the MRI volumes of 10 patients with right hemispheric lesions were flipped along the midsagittal plane [Grefkes et al., 2008b]. The data of an equivalent proportion of controls ($n = 6$) were processed in the same manner. Note that after the flipping procedure movement activation maps in the healthy control group are no longer specific for moving the left or right hand. That means that hemispheric differences in movement activation patterns are neglected in this study.

FMRI data

Images were processed using Statistical Parametric Mapping software (SPM5; Wellcome Trust Centre for Neuroimaging, University College London) for spatial preprocessing (realignment, spatial normalization, and spatial smoothing) and individual statistical analysis (cf. Supporting Information Methods). The following conditions were modelled in the design matrix: (1) movements of the affected (right) index finger, (2) movements of the unaffected (left) index finger, (3) instructions for moving the affected (right) index finger, and (4) instructions for moving the unaffected (left) index finger.

A laterality index (LI) was calculated for each subject to define the hemispheric lateralization of the fMRI BOLD signal during unimanual movements of the affected/right index finger [Carey et al., 2002; Cramer et al., 1997; Johansen-Berg et al., 2002]. The LI was computed by $[(C - I)/(C + I)]$, where C = the number of activated voxels within the contralateral (pre-) motor cortex (within Brodmann areas [BA] 4 and 6 according to the probabilistic cytoarchitectonic atlas provided by the SPM Anatomy toolbox) [Eickhoff et al., 2005] and I = the number of activated voxels within the ipsilateral BA 4 and 6 during movements of unilateral index finger, applying a threshold of $p < 0.001$ (uncorrected at the voxel level). An LI of "+1" is equivalent to a completely lateralized activation pattern to the contralateral motor areas, whereas an LI of "0" indicates an absolutely bilateral pattern.

Diffusion MRI data

The diffusion MRI data were analyzed using the FMRIB Software Library (FSL; Oxford Centre for Functional MRI of the Brain, University of Oxford).

Diffusion MRI parameters

Motion and eddy current correction were carried out using affine registration to the first nondiffusion weighted image [Jenkinson et al., 2002]. Data were skull-stripped using FMRIB's Brain Extraction Tool [Smith, 2002]. Subsequently, the three eigenvalues (λ_1, λ_2, and λ_3) and fractional anisotropy (FA) were calculated for each voxel using a diffusion tensor model [Basser et al., 1994; Basser and Pierpaoli, 1996]. The FA is often used as a quantitative biomarker for white matter integrity [Beaulieu, 2009], which is a scalar between 0 (i.e., complete isotropy) and 1 (i.e., complete anisotropy) describing the degree of diffusion anisotropy. The parallel diffusivity ($\lambda_{\parallel}$; also called axial diffusivity) is the primary eigenvalue (λ_1) of the diffusion tensor, which in white matter reflects the magnitude of water diffusion parallel to axons, and hence reflects axonal properties [Budde et al., 2009; Song et al., 2003; Zhang et al., 2009]. The perpendicular diffusivity ($\lambda_{\perp}$; also called radial diffusivity) is the average of the secondary (λ_2) and tertiary (λ_3) eigenvalues, and reflects the magnitude of diffusion orthogonal to the direction of the primary eigenvalue (i.e., axons). This parameter is related to properties of the myelin sheath [Song et al., 2003, 2005; Zhang et al., 2009].

Voxelwise Analysis of White Matter Tract

Tract-Based Spatial Statistics toolbox (TBSS) was used to perform voxelwise analyses of (1) the FA, (2) parallel diffusivity, and (3) perpendicular diffusivity data (see Supporting Information Methods for detailed procedures).

Voxelwise statistical analyses across subjects were carried out on the skeleton images of FA, parallel diffusivity, and perpendicular diffusivity, which were normalized into MNI standard space. We first performed a between-group analysis to compare patients and controls. Age of subjects was modeled as a nuisance regressor in order to control for age effects on white matter FA [Pfefferbaum et al., 2000]. Then, the FA skeleton images of the subjects were correlated with (1) the laterality index obtained from the fMRI contrast "movements of the affected index finger vs. rest" (patients) or "movements of the right index finger vs rest" (controls), respectively, and (2) motor scores obtained by the ARAT in patients. The purpose of these two analyses was to identify where in white matter FA was correlated with the laterality index or ARAT score. In subsequent region of interest analyses, we first verified the correlation results between white matter integrity (indexed by FA) and laterality index or ARAT scores by including "age of patients" and "lesion age" as nuisance regressors in multiple linear regression analyses. We then modeled both parallel and perpendicular diffusivities in multiple linear regression analyses to investigate the relationships between axonal or myelin damage and laterality index or ARAT scores.

Statistical analyses were performed with a nonparametric permutation test using 500 Monte Carlo simulations [Nichols and Holmes, 2002]. The statistical threshold was set at family-wise error (FWE) corrected clusterwise $P < 0.05$, based on the threshold-free cluster enhancement (TFCE) statistic image [Smith and Nichols, 2009]. Default TFCE parameters $H = 2$ and $E = 0.5$ were used.

Region of Interest Analyses

We first extracted the mean FA from the skeleton voxels showing significant correlations between FA and fMRI laterality index or ARAT scores, and carried out multiple

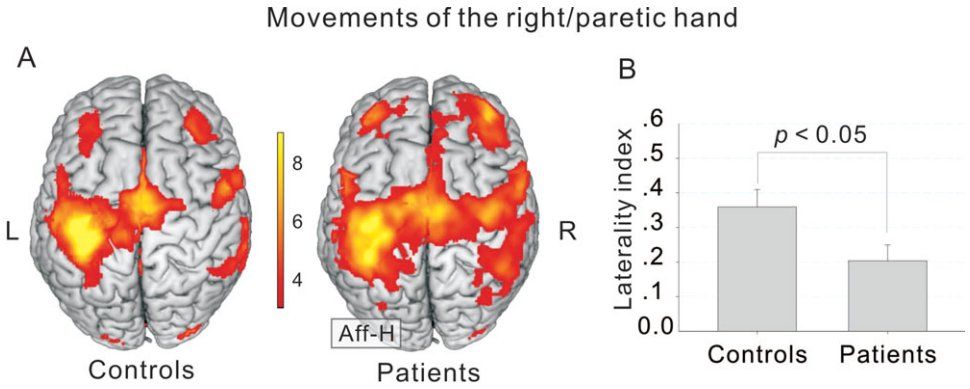

Figure 2.

Brain activity pattern during index finger movements of the right/paretic hand with maximum speed. Compared with controls, stroke patients showed abnormally enhanced activity in bilateral motor areas (**A**) and reduced laterality indices (**B**) when moving the affected hand. Aff-H, affected hemisphere. See also Supporting Information Table II for individual fMRI laterality indices.

linear regression analyses using FA, age of patients, and lesion age as independent variables and fMRI laterality index or ARAT scores as dependent variables. To analyze the relationship between pathological changes in parallel or perpendicular diffusivity and fMRI brain activity as well as motor performance of the affected hand, we extracted mean parallel and perpendicular diffusivities from the skeleton voxels showing significant correlations between FA and fMRI laterality index or ARAT scores. We finally performed multiple linear regression analyses using parallel diffusivity, perpendicular diffusivity, age of patients, and lesion age as independent variables and fMRI laterality index or ARAT scores as dependent variables. All regression analyses were performed with Statistical Product and Service Solutions software (SPSS; Chicago, IL).

Probabilistic Fiber Tracking

Statistically significant clusters from the TBSS analysis (see Fig. 3) were used as seed regions in a probabilistic multiple fiber tracing analysis [Behrens et al., 2007; Behrens et al., 2003a; Behrens et al., 2003b]. The clusters ($n = 10$) were deprojected to original diffusion MRI space of each patient and then used as a seed mask for the fiber tracking analysis. The tracking results were thresholded to include only those voxels that received more than 5.0×10^{-3} percent of the total streamlines sent out from the cluster masks used to trace the respective tract. The thresholded tracts were normalized to MNI standard space using the same deformation parameters derived from the normalization procedure of FA data and superimposed on each other yielding a summary map.

RESULTS

Behavioral Testings and fMRI

In the patients' group finger tapping frequencies of the paretic hand were significantly slower compared with healthy controls (patients: 3.01 ± 1.29 Hz; controls: 5.80 ± 0.35 Hz; $t(28) = 7.26$, $p < 0.001$; Supporting Information Table I). The fMRI group analysis revealed abnormally increased activity in bilateral motor cortex when patients tapped with their affected index finger compared with when the healthy controls tapped with maximum speed (see Fig. 2). In line with this finding, the laterality index computed for the patient group was significantly smaller than that of controls ($p < 0.05$; Supporting Information Table II), indicating a stronger engagement of ipsilateral (i.e., contralesional) relative to contralateral (i.e., ipsilesional) motor areas in patients. The laterality index for movements of the affected index finger also significantly correlated with motor performance as assessed by the ARAT ($r_s = 0.71$, $p < 0.05$, Table I). Furthermore, there was a strong trend towards significance for the correlation between finger tapping frequencies of the affected hand and the laterality index ($r = 0.39$, $p = 0.056$). In summary patients with stronger motor impairments were characterized by relatively increased activation in the contralesional motor areas when moving the affected index finger.

Voxelwise Analysis of White Matter Tracts

Patients vs. controls

Voxelwise comparison of diffusion MRI parameters between patients and controls showed reductions in FA and parallel diffusivity, as well as increases in perpendicular diffusivity in the patient group (FWE corrected, $p < 0.05$). The changes in diffusion MRI parameters in stroke patients were located in bilateral corticospinal tract (CST) and corona radiata as well as corpus callosum (CC). There was neither a significant increase in FA and parallel diffusivity nor a decrease in perpendicular diffusivity in patients compared with controls ($p > 0.05$).

Correlation of FA with fMRI laterality index and ARAT scores

In the patient group, the laterality index during movements of the affected hand was positively correlated with FA in four clusters comprising the middle and posterior region of the CC as well as the ipsilesional CST (Fig. 3A; FWE corrected, $p < 0.05$). Hence, patients with a lower laterality index (i.e., more bilateral activation pattern in motor areas) showed smaller FA values in these regions. ARAT scores positively correlated with FA values in a number of tracts located in the CC, bilateral CST, pons, and bilateral cerebellum (Fig. 3B). This means that patients with more severe motor deficits were characterized by smaller FA values in these regions. Note that only FA changes in the affected cerebral hemisphere, corpus callosum and brain stem correlated with the fMRI laterality index or the ARAT score in patients (see Fig. 3). Furthermore, clusters situated within the internal capsule (clusters 3, 4, and 6) showed a partial overlap with the summary lesion volume computed from the individual lesion maps (Supporting Information Fig. 1). In contrast, no significant correlations between FA and laterality index were observed for movements of the unaffected index finger ($p > 0.05$). The healthy control group showed no significant correlations (neither positive nor negative) between FA and fMRI laterality index during movements of the right or left index finger ($p > 0.05$). Hence, the significant correlations between behavioral scores, fMRI signal, and diffusion MRI parameters were specific to the group of subjects affected by ischemic lesions.

Region of interest analysis

Relation between FA and fMRI laterality index or ARAT score

We extracted the mean FA from the four clusters, where FA correlated with the laterality index (Fig. 3A), and the regions, where FA correlated with the ARAT scores (Fig. 3B). We first tested whether confounding variables like "age of patients" and "lesion age" influenced the correlations in these clusters. Multiple linear regression analyses demonstrated that FA in these regions was a significant predictor for both laterality index and ARAT scores ($p < 0.05$; see Beta coefficients in Table II) independent from patients' age or lesion age.

Relation of parallel diffusivity and perpendicular diffusivity to fMRI laterality index

Parallel and perpendicular diffusivities were extracted from the four clusters situated in the CC or ipsilesional CST (Fig. 3A). Linear regression analyses revealed that both parallel diffusivity (except for Cluster 3 located at inferior parts of the internal capsule) and perpendicular diffusivity were significant predictors for the laterality index in all four clusters ($p < 0.05$; see Beta coefficients in Table III). Parallel diffusivity was positively related to the laterality index (i.e., higher parallel diffusivity associated with higher laterality index), while perpendicular diffusivity showed an opposite relation (i.e., higher perpendicular diffusivity associated with lower laterality index). In addition, perpendicular diffusivity showed stronger relation to the fMRI laterality index (indicated by larger Beta values) than parallel diffusivity (see also Fig. 4 for visual demonstration). For example, in the multiple linear regression analysis for Cluster 1, the beta coefficient of parallel diffusivity was 0.461, which means that an increase of 1 standard deviation (SD) in parallel diffusivity may result in an increase of 0.461 SD in fMRI laterality index. The beta coefficient of perpendicular diffusivity was −0.778, which means that an increase of 1 SD in perpendicular diffusivity may lead to a decrease of 0.778 SD in fMRI laterality index. Note that neither FA, nor parallel and perpendicular diffusivity in the four clusters correlated with lesion age ($p > 0.05$), indicating that time since stroke did not significantly influence white matter abnormalities in our group of stroke patients. In addition, we separated the patients into two subgroups according to lesion age (i.e., less than or equal to eight weeks [median of the group] vs. greater than eight weeks). Independent-samples *t*-test did not find significant differences in diffusion MRI parameters in the four clusters between the two patient subgroups ($p > 0.05$), either.

Relation of parallel diffusivity and perpendicular diffusivity to ARAT scores

Parallel and perpendicular diffusivity were additionally extracted from the regions, where FA correlated with ARAT scores (shown in Fig. 3B). Multiple regression analyses showed that both parallel diffusivity and perpendicular diffusivity were significant predictors for ARAT scores ($p < 0.05$; Table III), albeit in opposite directions (i.e., parallel diffusivity: positive; perpendicular diffusivity: negative). Furthermore, perpendicular diffusivity showed stronger correlations than parallel diffusivity as indicated by larger Beta values (see also Fig. 5 for visual demonstration). Again, none of the FA, parallel and perpendicular diffusivity parameters in these regions significantly correlated with lesion age ($p > 0.05$).

Probabilistic Fiber Tracking

We used probabilistic fiber tracking and a multiple fiber model [Behrens et al., 2007] to identify which cortical regions were connected to the white matter clusters showing abnormalities in stroke patients. The multiple fiber model [Behrens et al., 2007] used for tracking analyses in this study provides advantages in sensitivity when tracking nondominant fibers, but does not dramatically change tractography results for the dominant fibers. This study

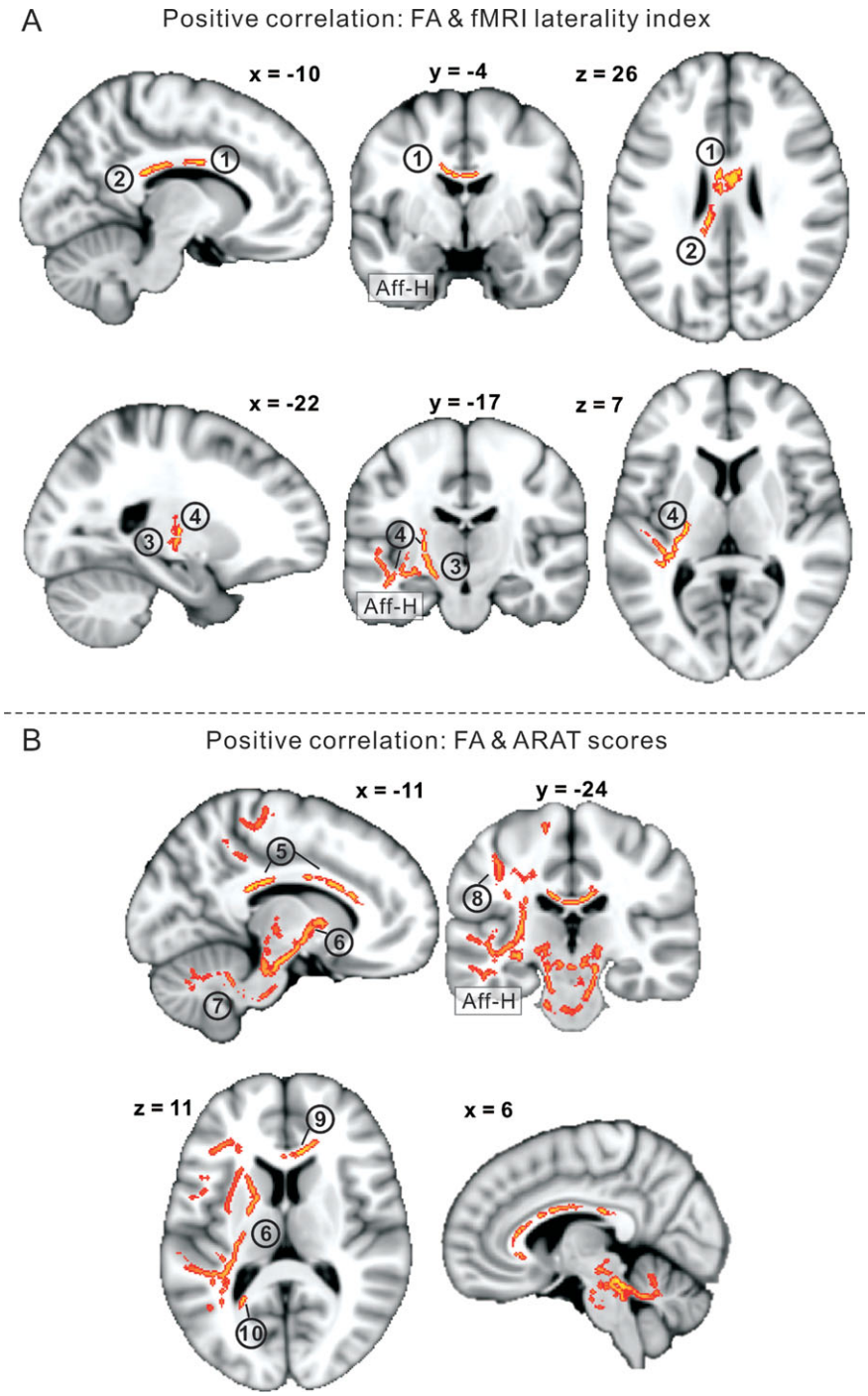

Figure 3.

Voxelwise correlation analyses between FA and fMRI laterality index as well as ARAT scores in patients ($n = 18$). FA values positively correlated with both the laterality index during movements of the affected index finger (**A**) and ARAT scores (**B**) ($p < 0.05$, FWE corrected at the cluster level). Shown are clusters in: 1 and 2, body of corpus callosum; 3, internal capsule; 4, posterior limb of internal capsule and adjacent inferior longitudinal fasciculus and fronto-occipital fasciculus; 5, body of corpus callosum; 6, internal capsule; 7, cortico-pontine-cerebellar tract; 8, superior longitudinal fasciculus; 9, genu of corpus callosum; 10, splenium of corpus callosum. Parts of cluster 3, 4, and 6 are within the lesion zone (Supporting Information Fig. 1). For visualization, clusters were "thickened" by applying spherical smoothing with 2 mm radius. Aff-H: Affected hemisphere.

TABLE II. Multiple linear regression analyses with fMRI laterality index or ARAT scores (FA)

	Regions	Diffusion MRI parameters	R^2	Beta
(A) Linear regression with LI	Cluster_1	FA	0.705**	3.039**
		Age		0.000
		Lesion age		0.002
	Cluster_2	FA	0.512*	2.753**
		Age		0.004
		Lesion age		−0.002
	Cluster_3	FA	0.556**	2.574**
		Age		0.000
		Lesion age		−0.001
	Cluster_4	FA	0.616**	2.919**
		Age		0.002
		Lesion age		−0.002
(B) Linear regression with ARAT scores	FA positively correlated with ARAT scores	FA	0.684**	194.342***
		Age		0.199
		Lesion age		−0.119

Multiple linear regression analyses with fMRI laterality index (A) or ARAT scores (B). The independent variables included FA, age of patients, and lesion age. Multiple regression analyses of these parameters well predicted laterality index or ARAT scores (indicated by significant R^2, $P < 0.05$). The regions are shown in Figure 3. Beta, standardized coefficients. LI, laterality index.
*$p < 0.05$.; **$p < 0.01$. ***$p < 0.001$.

especially focused on the corpus callosum as changes in transcallosal connections in stroke patients might impact on interhemispheric communication and activity levels of the unaffected hemisphere (Grefkes and Fink, 2011). We, therefore, restricted our tracking analyses to those clusters (Clusters 1 and 2 in Fig. 3) in the corpus callosum where we found both (i) correlations of FA with fMRI laterality indices and (ii) correlations of FA with motor performance measures (i.e., ARAT). The group results demonstrated that the tracts running through cluster 1 located in middle parts of the CC (Fig. 3A) connected to homologous regions in medial (M1, supplementary motor area (SMA)) and ventral frontal cortex (ventral premotor cortex, vPMC) and postcentral gyrus (primary somatosensory cortex) (Fig. 6A). The tracts passing Cluster 2 in posterior CC (Fig. 3A) linked to areas in medial superior parietal lobule (SPL), the temporoparietal junction (TPJ), superior and middle temporal gyrus, as well as precentral gyrus (corresponding to M1) (Fig. 6B). In addition, a summary mask computed from the MNI-normalized lesion volumes was superimposed onto the tractography results (Fig. 6 C,D) which revealed that the fiber tracts running through Clusters 1 and 2 in the CC were affected by the lesion zone. Hence, changes in CC integrity may be the consequence of direct damage to fibers originating from sensorimotor cortex, SMA, vPMC, and parietal cortex. The tractography results of the other 8 regions also depicted in Figure 3 are reported in the Supplementary Material (Supporting Information Figs. 2–9).

TABLE III. Multiple linear regression analyses with fMRI laterality index or ARAT scores (parallel and perpendicular diffusivities)

	Regions	Diffusion MRI parameters	R^2	Beta
(A) Linear regression with LI	Cluster_1	$\lambda_{\parallel}$	0.789**	0.461**
		$\lambda_{\perp}$		−0.778***
	Cluster_2	$\lambda_{\parallel}$	0.604**	0.656*
		$\lambda_{\perp}$		−1.029**
	Cluster_3	$\lambda_{\parallel}$	0.528*	0.205
		$\lambda_{\perp}$		−0.610*
	Cluster_4	$\lambda_{\parallel}$	0.659**	0.597*
		$\lambda_{\perp}$		−1.059**
(B) Linear regression with ARAT scores	FA positively correlated with ARAT scores	$\lambda_{\parallel}$	0.710**	0.530**
		$\lambda_{\perp}$		−0.930***

Multiple linear regression analyses with fMRI laterality index (A) or ARAT scores (B). The independent variables included parallel diffusivity, perpendicular diffusivity, age of patients, and lesion age. Multiple regression analyses of these parameters well predicted laterality index or ARAT scores (indicated by significant R^2, $p < 0.05$). The regions are shown in Figure 3. Beta, standardized coefficients. LI, laterality index. $\lambda\parallel$: parallel diffusivity. $\lambda\perp$: perpendicular diffusivity.
*$p < 0.05$; **$p < 0.01$; ***$p < 0.001$. See also Figures 4 and 5 for visual demonstration.

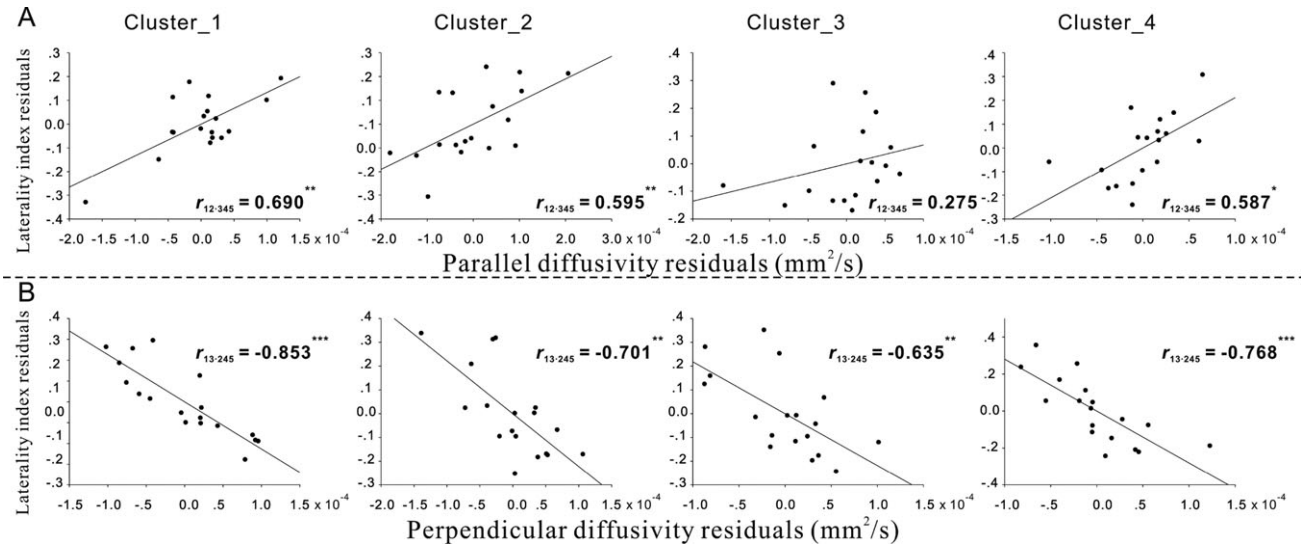

Figure 4.

Region of interest analyses: Partial correlation between fMRI laterality index and parallel diffusivity as well as perpendicular diffusivity. The parallel diffusivities (except for cluster 3) were positively correlated with the laterality index controlled for perpendicular diffusivity, age of patients, and lesion age (**A**), but the perpendicular diffusivities were negatively correlated with the laterality index controlled for parallel diffusivity, age of patients, and lesion age (**B**). The locations of the four clusters are shown in Figure 3A. Variables: 1, laterality index; 2, parallel diffusivity; 3, perpendicular diffusivity; 4, age of patients; 5, lesion age. *$p < 0.05$, **$p < 0.01$, ***$p < 0.001$.

DISCUSSION

The novel finding of this study is that white matter abnormalities in the corpus callosum in stroke patients are associated with poor motor recovery and relatively increased movement-related BOLD activity in contralesional motor areas. Changes in white matter encompassed both decreased parallel diffusivity (possibly reflecting axonal injury) and increased perpendicular diffusivity (likely reflecting destruction of myelin sheath). In addition, probabilistic fiber tracking analyses revealed that subregions of the CC, where FA significantly correlated with the fMRI laterality index and ARAT scores, connected to cortical midline structures (sensorimotor cortex, SMA, SPL), as well as

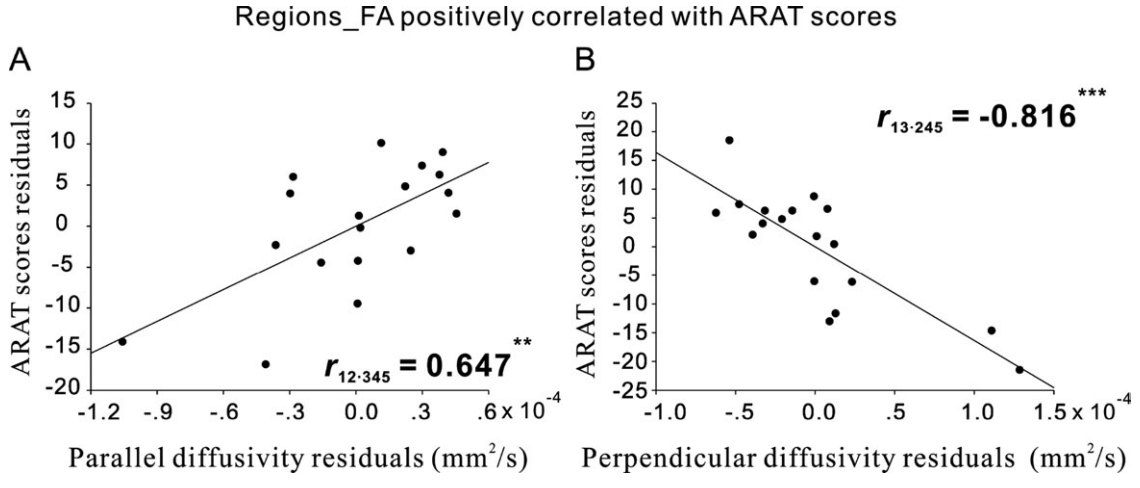

Figure 5.

Region of interest analyses: Partial correlation between ARAT scores and parallel diffusivity as well as perpendicular diffusivity. The parallel diffusivities in the regions shown in Fig. 3B were positively correlated with ARAT scores controlled for perpendicular diffusivity, age of patients, and lesion age (**A**), but the perpendicular diffusivities were negatively correlated with ARAT scores controlled for perpendicular diffusivity, age of patients, and lesion age (**B**). Variables: 1, ARAT scores; 2, parallel diffusivity; 3, perpendicular diffusivity; 4, age of patients; 5, lesion age. **$p < 0.01$, ***$p < 0.001$.

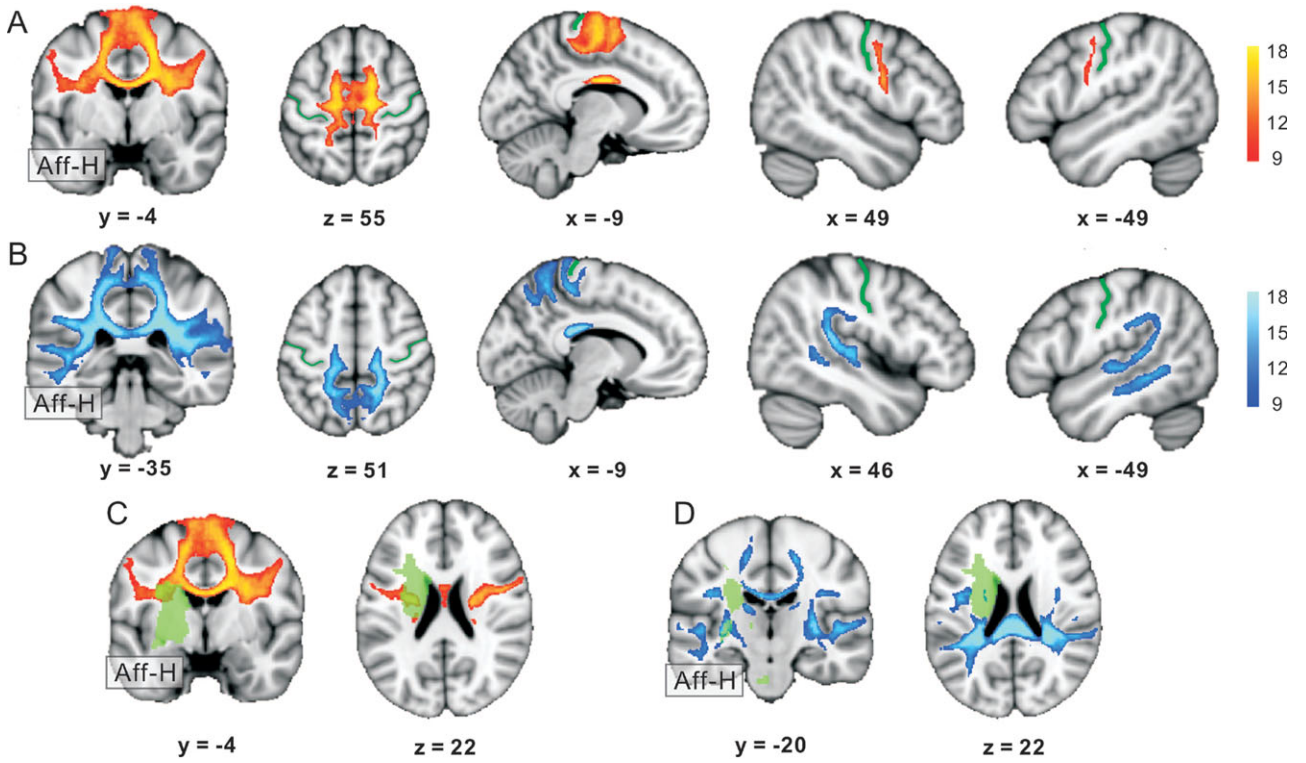

Figure 6.

Probabilistic fiber tracking with seeds in the corpus callosum (thresholded at more than eight subjects). The area covered by cluster 1 (seed region, shown in Fig. 3A) in the corpus callosum connected to the medial and ventral side of the precentral gyrus as well as the postcentral gyrus (corresponding to M1, SMA, vPMC, and primary somatosensory cortex; **A**). Cluster 2 (seed region, shown in Fig. 3A) in the corpus callosum connected to the medial side of both superior parietal lobules, temporal cortices, and precentral gyri (corresponding to M1) (**B**). The green area indicates the lesion volume of the sample of patients in this study. The stroke lesions affected the white matter fibers connecting to bilateral SMA and vPMC (**C**). The posterior part of the lesions also affected the fibers connecting to the parietal lobules bilaterally (**D**). Aff-H, affected hemisphere. The green line in the figure indicates the central sulcus. The color bar indicates the number of superimposed tract masks of the patients (red/blue: representations in nine patients; yellow/light blue: representations in 18 patients).

to lateral premotor (vPMC) and multimodal cortex along the TPJ. The data suggest that a stroke induced brain injury may result in destructive processes distant to the primary lesion site leading to both degradation of axons and myelin sheath in the CC which might ultimately influence cortical reorganization and motor recovery.

Diffusion MRI Detected Microstructural Changes in White Matter and Its Functional Implications

Our data are consistent with the results of previous longitudinal studies in stroke patients showing that reduced FA resulted from (i) an early decrease in parallel diffusivity and (ii) a later increase in perpendicular diffusivity [Thomalla et al., 2005; Yu et al., 2009]. Animal studies using both noninvasive diffusion MRI and invasive immunohistochemical staining techniques revealed that that a reduction of parallel diffusivity is associated with axonal damage, whereas an increase of perpendicular diffusivity largely relates to reduced integrity of myelin sheath [Budde et al., 2009; Kerschensteiner et al., 2005; Song et al., 2003, 2005; Sun et al., 2006, 2008; Zhang et al., 2009]. These observations are consistent with the results of previous animal models showing that ischemia may cause both axon and myelin damage in white matter [Arai and Lo, 2009; Medana and Esiri, 2003; Valeriani et al., 2000; Wakita et al., 2002]. However, it should be noted that the interpretation of parallel and perpendicular diffusivities with respect to their neural substrates is not entirely clear. It has been suggested that changes in parallel and perpendicular diffusivities may differentiate axon and myelin damage in mouse optic nerve after retinal ischemia [Song et al., 2003; Sun et al., 2008]. Using histology, Song et al. [2005] demonstrated in a mouse model that increases in perpendicular diffusivity in corpus callosum are associated with demyelination. In contrast, using a Wallerian degeneration model in rat spinal cord after dorsal root axotomy, a recent study

suggested that progressive increases in perpendicular diffusivity result from clearance of myelin following axonal degeneration [Zhang et al., 2009]. As in our study changes in perpendicular diffusivity in CC were co-localized with changes in parallel diffusivity (Figs. 4 and 5) and were structurally connected to the primary lesion site, we suggest that the pathology underlying these changes rather reflects Wallerian degeneration including loss of myelin sheath. Taken together, the interpretation of parallel and perpendicular diffusivities in human brains still needs clarification [Wheeler-Kingshott and Cercignani, 2009].

Furthermore, not all damages to white matter can be detected by conventional structural imaging, especially in patients where thrombolysis was administered in the acute phase due to total blockage of the middle cerebral artery. Here, T1 and FLAIR images might appear normal although a number of neurons may have died during acute ischemia while glial cells less sensitive to ischemia survived [Baron, 2005]. Although the lesion pattern in our group of patients somewhat resembles that observed in patients with severe stroke which did not respond to thrombolysis [Seitz et al., 2009], only 2 out of 18 patients included in the present study received thrombolysis (Table I). In all other patients, the NIHSS in the acute phase was not excessively higher (indicating a relevant middle cerebral artery (MCA) occlusion) than the NIHSS assessed when scanning the patients. It therefore appears unlikely that thrombolysis (spontaneous or after recanalization therapy) significantly influenced our results. In addition, previous studies with stroke patients have demonstrated that also white matter in the contralesional cerebellum remote to infarct zone may show abnormalities in stroke patients [Pantano et al., 1986; Pappata et al., 1990]. Consistent with these data, we found that the FA of white matter in the pons and the contralesional cerebellum was correlated with ARAT scores in patients (Fig. 3B).

Enhanced neural activity in contralesional areas in stroke patients might also result from differences in task difficulty and attentional load, when moving the stroke-affected hand. For example, it was shown that activation in ipsilateral sensorimotor cortex and premotor cortex increased with higher task difficulty [Johansen-Berg et al., 2002; Seidler et al., 2004]. As in this study difficulty levels were matched between patients and controls, increased activity in the contralesional hemisphere (as indexed by lower laterality indices in the patients' group) is unlikely to result from differences in task difficulty. Our results are thus consistent with the findings of Johansen-Berg et al. [2002] who showed that the fMRI laterality index correlates with motor impairment in stroke patients. In addition, a more recent study showed that there is a linear increase of brain activity with higher finger tapping frequencies in the ipsilateral/contralesional premotor cortex and sensorimotor cortex in stroke patients but not in healthy subjects [Riecker et al., 2010]. These data suggest that changes in ipsilateral/contralesional motor areas are related to functional reorganization in stroke patients.

Integrity of the Corpus Callosum and Motor Deficits

The novel finding of this study was that white matter abnormalities in CC correlated with a more bilateralized brain activation pattern in motor areas during movements of the affected hand in patients with stronger motor deficits. The CC enables interhemispheric interactions related to sensory, motor, and cognitive functions [Doron and Gazzaniga, 2008; Gazzaniga, 2000]. Recent diffusion MRI studies revealed that structural changes of the CC coincide with differences in behavioral performance of healthy subjects or patients with white matter damage [Bhadelia et al., 2009; Bonzano et al., 2008; Johansen-Berg et al., 2007; Lenzi et al., 2007; Putnam et al., 2008]. For example, lower FA in anterior CC was associated with poor performance and higher activity of right (nondominant) BA 44 in a verbal encoding/memory task [Putnam et al., 2008] probably reflecting less effective transcallosal inhibition originating from left (dominant) BA 44, thereby interfering with task performance. A similar relationship between CC integrity, contralesional (relative to ipsilesional) motor areas activity and behavioral performance was demonstrated in this present study. The fact that FA variability did not predict motor performance and lateralization of BOLD activity in the healthy control group implies that structural and functional changes were indeed specific to our group of subcortical stroke patients.

The fiber tracking analysis of the present study together with other recent diffusion tractography studies revealed that the middle part of the CC is connected to motor areas, while the posterior part is linked to parietal and temporal cortex [Chao et al., 2009; Hofer and Frahm, 2006; Westerhausen et al., 2009]. Of note, network simulation studies showed that lesions to regions identified by our tracking analysis may produce widespread and bihemispheric disturbances in cortico-cortical interactions [Alstott et al., 2009; Honey and Sporns, 2008]. Hence, damage to transcallosal fibres of such "connector hubs" might explain the widespread changes in BOLD activity as found in this study.

Disturbed interhemispheric interactions after stroke were also observed at the level of the primary motor cortices by means of paired-pulse TMS [Butefisch et al., 2008; Shimizu et al., 2002]. Murase et al. found that in stroke patients contralesional M1 may exert an abnormally enhanced inhibitory drive onto ipsilesional M1 during movement preparation which is not found in healthy subjects [Murase et al., 2004]. Similar changes in M1-M1 coupling were found employing models of effective connectivity to fMRI data [Grefkes et al., 2008b]. Such analyses furthermore demonstrated reduced interhemispheric coupling among premotor areas such as both SMA and vPMC in stroke patients compared with healthy controls [Grefkes et al., 2008b; Wang et al., 2011], which is in line with the structural abnormalities in transcallosal SMA fibers observed in the present study. Studies in monkeys suggested that the vPMC is particularly related to finger

movements and might also play an important role in motor recovery [Dancause et al., 2005; Frost et al., 2003; Gentilucci et al., 1988; Shimazu et al., 2004; Wang et al., 2011]. Anatomical tracing studies demonstrated widespread transcallosal connections of the SMA and vPMC with various motor areas in the opposite hemisphere [Dancause et al., 2007; Rouiller et al., 1994]. In addition, recent connectivity analyses of the motor network revealed that not only contralateral M1 but also contralateral SMA and vPMC exert negative influences over ipsilateral M1, when healthy subjects or stroke patients perform unilateral hand movements [Grefkes et al., 2008a; Grefkes et al., 2008b; Grefkes et al., 2010; Rehme et al., 2011; Wang et al., 2011]. Therefore, reduced influences of ipsilesional SMA and vPMC on contralesional motor areas might contribute to abnormally increased neural activity in the contralesional (relative to ipsilesional) motor areas apart from intracortical changes within the M1 region [Butefisch et al., 2003; Talelli et al. 2006]. A recent fMRI study demonstrated that increased activation in the temporoparietal junction (TPJ) was associated with longer reaction time under conditions of higher uncertainty, and was positively correlated with reaction time [Jakobs et al., 2009]. These data suggest that the TPJ might play an important role in predictive motor coding. Therefore, malfunction of connectivity of the TPJ might result in worse motor performance in stroke patients.

It is important to note, however, that the present results do not provide information regarding the specific role (i.e., beneficial or detrimental) of the contralesional motor cortex in stroke patients, but rather suggest that the structural abnormality in tracts that connect bilateral motor areas might influence functional reorganization of the contralesional motor areas. For example, axonal and myelin damage in the CC might result in decreased inhibition of contralesional sensorimotor areas similar to what has been observed in fMRI models of connectivity [Grefkes et al., 2008b; Grefkes and Fink, 2011]. This hypothesis is also supported by a recent diffusion MRI study investigating anatomical and functional organization of the human CC, showing that FA in a part of CC, which is linked to the M1 hand representation, was correlated with the degree of interhemispheric inhibition (measured by TMS) [Wahl et al., 2007]. In other words, lower FA was associated with weaker interhemispheric inhibition. However, noninvasive brain stimulation studies aiming at reducing cortical excitability of contralesional motor areas to improve motor functions have found beneficial effects only after transient downregulation of contralesional M1 [Grefkes et al., 2010; Mansur et al., 2005; Nowak et al., 2008]. In contrast, TMS interference with contralesional dorsal PMC activity was demonstrated to deteriorate motor performance of the paretic hand, suggesting a supportive role for recovered hand function after stroke [Johansen-Berg et al., 2002]. In summary, more studies using a multimodal approach to establish structure-function relationships after stroke are needed to further our understanding of the role of contralesional areas in stroke recovery [Bestmann et al., 2010; Grefkes and Fink, 2011; Hummel and Cohen, 2006; Nowak et al., 2009].

CONCLUSIONS

Our results demonstrated that changes in parallel and perpendicular diffusivities in the corpus callosum and corticospinal tract are related to interhemispheric reorganization in motor areas and motor deficits in stroke patients. This suggests that the structural integrity of the corpus callosum is a relevant factor influencing functional recovery after stroke. Further clarification of the neurobiological processes underlying changes in parallel and perpendicular diffusivities in stroke patients may contribute to a better understanding of the mechanisms driving functional reorganization after stroke.

ACKNOWLEDGMENTS

The authors are grateful to the patients and healthy subjects who participated in the study. We would also like to thank Dr. Michael von Mengershausen, Timm Wetzel, and Kurt Wittenberg, for their continued and valuable support.

REFERENCES

Alstott J, Breakspear M, Hagmann P, Cammoun L, Sporns O (2009): Modeling the impact of lesions in the human brain. PLoS Comput Biol 5:e1000408.

Arai K, Lo EH (2009): Experimental models for analysis of oligodendrocyte pathophysiology in stroke. Exp Transl Stroke Med 1:6.

Baron JC (2005): Stroke research in the modern era: Images versus dogmas. Cerebrovasc Dis 20:154–163.

Basser PJ, Mattiello J, LeBihan D (1994): Estimation of the effective self-diffusion tensor from the NMR spin echo. J Magn Reson B 103:247–254.

Basser PJ, Pierpaoli C (1996): Microstructural and physiological features of tissues elucidated by quantitative-diffusion-tensor MRI. J Magn Reson B 111:209–219.

Beaulieu C (2009): The biological basis of diffusion anisotropy. In: Johansen-Berg H, Behrens TEJ, editors. Diffusion MRI: From Quantitative Measurement to In-Vivo Neuroanatomy. London: Elsevier.

Behrens TE, Berg HJ, Jbabdi S, Rushworth MF, Woolrich MW (2007): Probabilistic diffusion tractography with multiple fibre orientations: What can we gain? Neuroimage 34:144–155.

Behrens TE, Johansen-Berg H, Woolrich MW, Smith SM, Wheeler-Kingshott CA, Boulby PA, Barker GJ, Sillery EL, Sheehan K, Ciccarelli O, et al. (2003a): Non-invasive mapping of connections between human thalamus and cortex using diffusion imaging. Nat Neurosci 6:750–757.

Behrens TE, Woolrich MW, Jenkinson M, Johansen-Berg H, Nunes RG, Clare S, Matthews PM, Brady JM, Smith SM (2003b): Characterization and propagation of uncertainty in diffusion-weighted MR imaging. Magn Reson Med 50:1077–1088.

Bestmann S, Swayne O, Blankenburg F, Ruff CC, Teo J, Weiskopf N, Driver J, Rothwell JC, Ward NS (2010): The role of

contralesional dorsal premotor cortex after stroke as studied with concurrent TMS-fMRI. J Neurosci 30:11926–11937.

Bhadelia RA, Price LL, Tedesco KL, Scott T, Qiu WQ, Patz S, Folstein M, Rosenberg I, Caplan LR, Bergethon P (2009): Diffusion tensor imaging, white matter lesions, the corpus callosum, and gait in the elderly. Stroke 40:3816–3820.

Bonzano L, Tacchino A, Roccatagliata L, Abbruzzese G, Mancardi GL, Bove M (2008): Callosal contributions to simultaneous bimanual finger movements. J Neurosci 28:3227–3233.

Budde MD, Xie M, Cross AH, Song SK (2009): Axial diffusivity is the primary correlate of axonal injury in the experimental autoimmune encephalomyelitis spinal cord: A quantitative pixelwise analysis. J Neurosci 29:2805–2813.

Butefisch CM, Netz J, Wessling M, Seitz RJ, Homberg V. (2003): Remote changes in cortical excitability after stroke. Brain 126(Part 2):470–481.

Butefisch CM, Wessling M, Netz J, Seitz RJ, Homberg V (2008): Relationship between interhemispheric inhibition and motor cortex excitability in subacute stroke patients. Neurorehabil Neural Repair 22:4–21.

Carey JR, Kimberley TJ, Lewis SM, Auerbach EJ, Dorsey L, Rundquist P, Ugurbil K (2002): Analysis of fMRI and finger tracking training in subjects with chronic stroke. Brain 125(Part 4):773–788.

Chao YP, Cho KH, Yeh CH, Chou KH, Chen JH, Lin CP (2009): Probabilistic topography of human corpus callosum using cytoarchitectural parcellation and high angular resolution diffusion imaging tractography. Hum Brain Mapp 30:3172–3187.

Cramer SC (2008): Repairing the human brain after stroke. I. Mechanisms of spontaneous recovery. Ann Neurol 63:272–287.

Cramer SC, Nelles G, Benson RR, Kaplan JD, Parker RA, Kwong KK, Kennedy DN, Finklestein SP, Rosen BR (1997): A functional MRI study of subjects recovered from hemiparetic stroke. Stroke 28:2518–2527.

Dancause N, Barbay S, Frost SB, Mahnken JD, Nudo RJ (2007): Interhemispheric connections of the ventral premotor cortex in a new world primate. J Comp Neurol 505:701–715.

Dancause N, Barbay S, Frost SB, Plautz EJ, Chen D, Zoubina EV, Stowe AM, Nudo RJ (2005): Extensive cortical rewiring after brain injury. J Neurosci 25:10167–10179.

De Stefano N, Narayanan S, Francis GS, Arnaoutelis R, Tartaglia MC, Antel JP, Matthews PM, Arnold DL (2001): Evidence of axonal damage in the early stages of multiple sclerosis and its relevance to disability. Arch Neurol 58:65–70.

Doron KW, Gazzaniga MS (2008): Neuroimaging techniques offer new perspectives on callosal transfer and interhemispheric communication. Cortex 44:1023–1029.

Eickhoff SB, Stephan KE, Mohlberg H, Grefkes C, Fink GR, Amunts K, Zilles K (2005): A new SPM toolbox for combining probabilistic cytoarchitectonic maps and functional imaging data. Neuroimage 25:1325–1335.

Frost SB, Barbay S, Friel KM, Plautz EJ, Nudo RJ (2003): Reorganization of remote cortical regions after ischemic brain injury: A potential substrate for stroke recovery. J Neurophysiol 89:3205–3214.

Gazzaniga MS. (2000): Cerebral specialization and interhemispheric communication: Does the corpus callosum enable the human condition? Brain 123 (Part 7):1293–1326.

Gentilucci M, Fogassi L, Luppino G, Matelli M, Camarda R, Rizzolatti G (1988): Functional organization of inferior area 6 in the macaque monkey. I. Somatotopy and the control of proximal movements. Exp Brain Res 71:475–490.

Grefkes C, Eickhoff SB, Nowak DA, Dafotakis M, Fink GR. (2008a): Dynamic intra- and interhemispheric interactions during unilateral and bilateral hand movements assessed with fMRI and DCM. Neuroimage 41:1382–1394.

Grefkes C, Fink G (2011): Reorganization of cerebral networks after stroke: New insights from neuroimaging using connectivity approaches. Brain 134:1264–1276

Grefkes C, Nowak DA, Eickhoff SB, Dafotakis M, Kust J, Karbe H, Fink GR (2008b): Cortical connectivity after subcortical stroke assessed with functional magnetic resonance imaging. Ann Neurol 63:236–246.

Grefkes C, Nowak DA, Wang LE, Dafotakis M, Eickhoff SB, Fink GR (2010): Modulating cortical connectivity in stroke patients by rTMS assessed with fMRI and dynamic causal modelling. Neuroimage 50:233–242.

Hofer S, Frahm J (2006): Topography of the human corpus callosum revisited—Comprehensive fiber tractography using diffusion tensor magnetic resonance imaging. Neuroimage 32:989–994.

Honey CJ, Sporns O (2008): Dynamical consequences of lesions in cortical networks. Hum Brain Mapp 29:802–809.

Hummel F, Celnik P, Giraux P, Floel A, Wu WH, Gerloff C, Cohen LG. (2005): Effects of non-invasive cortical stimulation on skilled motor function in chronic stroke. Brain 128(Part 3):490–499.

Hummel FC, Cohen LG (2006): Non-invasive brain stimulation: A new strategy to improve neurorehabilitation after stroke? Lancet Neurol 5:708–712.

Jakobs O, Wang LE, Dafotakis M, Grefkes C, Zilles K, Eickhoff SB (2009): Effects of timing and movement uncertainty implicate the temporo-parietal junction in the prediction of forthcoming motor actions. Neuroimage 47:667–677.

Jang SH, Bai D, Son SM, Lee J, Kim DS, Sakong J, Kim DG, Yang DS (2008): Motor outcome prediction using diffusion tensor tractography in pontine infarct. Ann Neurol 64:460–465.

Jenkinson M, Bannister P, Brady M, Smith S (2002): Improved optimization for the robust and accurate linear registration and motion correction of brain images. Neuroimage 17:825–841.

Johansen-Berg H, Della-Maggiore V, Behrens TE, Smith SM, Paus T (2007): Integrity of white matter in the corpus callosum correlates with bimanual co-ordination skills. Neuroimage 36 (Suppl 2):T16–T21.

Johansen-Berg H, Rushworth MF, Bogdanovic MD, Kischka U, Wimalaratna S, Matthews PM (2002): The role of ipsilateral premotor cortex in hand movement after stroke. Proc Natl Acad Sci USA 99:14518–14523.

Kerschensteiner M, Schwab ME, Lichtman JW, Misgeld T (2005): In vivo imaging of axonal degeneration and regeneration in the injured spinal cord. Nat Med 11:572–577.

Lenzi D, Conte A, Mainero C, Frasca V, Fubelli F, Totaro P, Caramia F, Inghilleri M, Pozzilli C, Pantano P (2007): Effect of corpus callosum damage on ipsilateral motor activation in patients with multiple sclerosis: A functional and anatomical study. Hum Brain Mapp 28:636–644.

Lindenberg R, Renga V, Zhu LL, Betzler F, Alsop D, Schlaug G (2010): Structural integrity of corticospinal motor fibers predicts motor impairment in chronic stroke. Neurology 74:280–287.

Mansur CG, Fregni F, Boggio PS, Riberto M, Gallucci-Neto J, Santos CM, Wagner T, Rigonatti SP, Marcolin MA, Pascual-Leone A (2005): A sham stimulation-controlled trial of rTMS of the

unaffected hemisphere in stroke patients. Neurology 64:1802–1804.

Medana IM, Esiri MM (2003): Axonal damage: A key predictor of outcome in human CNS diseases. Brain 126(Part 3):515–530.

Murase N, Duque J, Mazzocchio R, Cohen LG (2004): Influence of interhemispheric interactions on motor function in chronic stroke. Ann Neurol 55:400–409.

Newton JM, Ward NS, Parker GJ, Deichmann R, Alexander DC, Friston KJ, Frackowiak RS (2006): Non-invasive mapping of corticofugal fibres from multiple motor areas—Relevance to stroke recovery. Brain 129(Part 7):1844–1858.

Nichols TE, Holmes AP (2002): Nonparametric permutation tests for functional neuroimaging: A primer with examples. Hum Brain Mapp 15:1–25.

Nowak DA, Grefkes C, Ameli M, Fink GR (2009): Interhemispheric competition after stroke: Brain stimulation to enhance recovery of function of the affected hand. Neurorehabil Neural Repair 23:641–656.

Nowak DA, Grefkes C, Dafotakis M, Eickhoff S, Kust J, Karbe H, Fink GR (2008): Effects of low-frequency repetitive transcranial magnetic stimulation of the contralesional primary motor cortex on movement kinematics and neural activity in subcortical stroke. Arch Neurol 65:741–747.

Oldfield RC (1971): The assessment and analysis of handedness: The Edinburgh inventory. Neuropsychologia 9:97–113.

Pantano P, Baron JC, Samson Y, Bousser MG, Derouesne C, Comar D (1986): Crossed cerebellar diaschisis. Further studies. Brain 109 (Part 4):677–694.

Pappata S, Mazoyer B, Tran Dinh S, Cambon H, Levasseur M, Baron JC (1990): Effects of capsular or thalamic stroke on metabolism in the cortex and cerebellum: A positron tomography study. Stroke 21:519–524.

Petzold A, Eikelenboom MJ, Keir G, Grant D, Lazeron RH, Polman CH, Uitdehaag BM, Thompson EJ, Giovannoni G (2005): Axonal damage accumulates in the progressive phase of multiple sclerosis: Three year follow up study. J Neurol Neurosurg Psychiatry 76:206–211.

Pfefferbaum A, Sullivan EV, Hedehus M, Lim KO, Adalsteinsson E, Moseley M (2000): Age-related decline in brain white matter anisotropy measured with spatially corrected echo-planar diffusion tensor imaging. Magn Reson Med 44:259–268.

Putnam MC, Wig GS, Grafton ST, Kelley WM, Gazzaniga MS (2008): Structural organization of the corpus callosum predicts the extent and impact of cortical activity in the nondominant hemisphere. J Neurosci 28:2912–2918.

Rehme AK, Eickhoff SB, Wang LE, Fink GR, Grefkes C (2011): Dynamic causal modeling of cortical activity from the acute to the chronic stage after stroke. Neuroimage 55:1147–1158.

Riecker A, Groschel K, Ackermann H, Schnaudigel S, Kassubek JR, Kastrup A (2010): The role of the unaffected hemisphere in motor recovery after stroke. Hum Brain Mapp 31:1017–1029.

Rouiller EM, Babalian A, Kazennikov O, Moret V, Yu XH, Wiesendanger M (1994): Transcallosal connections of the distal forelimb representations of the primary and supplementary motor cortical areas in macaque monkeys. Exp Brain Res 102:227–243.

Schaechter JD, Fricker ZP, Perdue KL, Helmer KG, Vangel MG, Greve DN, Makris N (2009): Microstructural status of ipsilesional and contralesional corticospinal tract correlates with motor skill in chronic stroke patients. Hum Brain Mapp 30:3461–3474.

Schaechter JD, Perdue KL, Wang R (2008): Structural damage to the corticospinal tract correlates with bilateral sensorimotor cortex reorganization in stroke patients. Neuroimage 39:1370–1382.

Seidler RD, Noll DC, Thiers G (2004): Feedforward and feedback processes in motor control. Neuroimage 22:1775–1783.

Seitz RJ, Sondermann V, Wittsack HJ, Siebler M (2009): Lesion patterns in successful and failed thrombolysis in middle cerebral artery stroke. Neuroradiology 51:865–871.

Shimazu H, Maier MA, Cerri G, Kirkwood PA, Lemon RN (2004): Macaque ventral premotor cortex exerts powerful facilitation of motor cortex outputs to upper limb motoneurons. J Neurosci 24:1200–1211.

Shimizu T, Hosaki A, Hino T, Sato M, Komori T, Hirai S, Rossini PM (2002): Motor cortical disinhibition in the unaffected hemisphere after unilateral cortical stroke. Brain 125(Part 8):1896–1907.

Smith SM (2002): Fast robust automated brain extraction. Hum Brain Mapp 17:143–155.

Smith SM, Nichols TE (2009): Threshold-free cluster enhancement: addressing problems of smoothing, threshold dependence and localisation in cluster inference. Neuroimage 44:83–98.

Song SK, Sun SW, Ju WK, Lin SJ, Cross AH, Neufeld AH (2003): Diffusion tensor imaging detects and differentiates axon and myelin degeneration in mouse optic nerve after retinal ischemia. Neuroimage 20:1714–1722.

Song SK, Yoshino J, Le TQ, Lin SJ, Sun SW, Cross AH, Armstrong RC (2005): Demyelination increases radial diffusivity in corpus callosum of mouse brain. Neuroimage 26:132–140.

Stinear CM, Barber PA, Smale PR, Coxon JP, Fleming MK, Byblow WD (2007): Functional potential in chronic stroke patients depends on corticospinal tract integrity. Brain 130(Part 1):170–180.

Sun SW, Liang HF, Cross AH, Song SK (2008): Evolving Wallerian degeneration after transient retinal ischemia in mice characterized by diffusion tensor imaging. Neuroimage 40:1–10.

Sun SW, Liang HF, Trinkaus K, Cross AH, Armstrong RC, Song SK (2006): Noninvasive detection of cuprizone induced axonal damage and demyelination in the mouse corpus callosum. Magn Reson Med 55:302–308.

Talelli P, Rothwell J (2006): Does brain stimulation after stroke have a future? Curr Opin Neurol 19:543–550.

Thomalla G, Glauche V, Koch MA, Beaulieu C, Weiller C, Rother J (2004): Diffusion tensor imaging detects early Wallerian degeneration of the pyramidal tract after ischemic stroke. Neuroimage 22:1767–1774.

Thomalla G, Glauche V, Weiller C, Rother J (2005): Time course of wallerian degeneration after ischaemic stroke revealed by diffusion tensor imaging. J Neurol Neurosurg Psychiatry 76:266–268.

Valeriani V, Dewar D, McCulloch J (2000): Quantitative assessment of ischemic pathology in axons, oligodendrocytes, and neurons: Attenuation of damage after transient ischemia. J Cereb Blood Flow Metab 20:765–771.

Volpe JJ (2001): Neurobiology of periventricular leukomalacia in the premature infant. Pediatr Res 50:553–562.

Wahl M, Lauterbach-Soon B, Hattingen E, Jung P, Singer O, Volz S, Klein JC, Steinmetz H, Ziemann U (2007): Human motor corpus callosum: topography, somatotopy, and link between microstructure and function. J Neurosci 27:12132–12138.

Wakita H, Tomimoto H, Akiguchi I, Matsuo A, Lin JX, Ihara M, McGeer PL (2002): Axonal damage and demyelination in the white matter after chronic cerebral hypoperfusion in the rat. Brain Res 924:63–70.

Wang LE, Fink GR, Diekhoff S, Rehme AK, Eickhoff SB, Grefkes C (2011): Noradrenergic enhancement improves motor network connectivity in stroke patients. Ann Neurol 69:375–388.

Ward NS, Newton JM, Swayne OB, Lee L, Thompson AJ, Greenwood RJ, Rothwell JC, Frackowiak RS (2006): Motor system activation after subcortical stroke depends on corticospinal system integrity. Brain 129(Part 3):809–819.

Westerhausen R, Gruner R, Specht K, Hugdahl K (2009): Functional relevance of interindividual differences in temporal lobe callosal pathways: A DTI tractography study. Cereb Cortex 19:1322–1329.

Wheeler-Kingshott CA, Cercignani M (2009): About "axial" and "radial" diffusivities. Magn Reson Med 61:1255–1260.

Yozbatiran N, Der-Yeghiaian L, Cramer SC (2008): A standardized approach to performing the action research arm test. Neurorehabil Neural Repair 22:78–90.

Yu C, Zhu C, Zhang Y, Chen H, Qin W, Wang M, Li K (2009): A longitudinal diffusion tensor imaging study on Wallerian degeneration of corticospinal tract after motor pathway stroke. Neuroimage 47:451–458.

Zhang J, Jones M, DeBoy CA, Reich DS, Farrell JA, Hoffman PN, Griffin JW, Sheikh KA, Miller MI, Mori S, et al. (2009): Diffusion tensor magnetic resonance imaging of Wallerian degeneration in rat spinal cord after dorsal root axotomy. J Neurosci 29:3160–3171.